Available online at www.sciencedirect.com
ScienceDirect
Journal of Sound and Vibration 308 (2007) 431–440
JOURNAL OF SOUND AND VIBRATION
www.elsevier.com/locate/jsvi

Mathematical models of gear rattle in Roots blower vacuum pumps

Joanna Mason*, Martin Homer, R. Eddie Wilson

Bristol Centre for Applied Nonlinear Mathematics, University of Bristol, Bristol BS8 1TR, UK

Accepted 28 March 2007
The peer review of this article was organised by the Guest Editor
Available online 4 June 2007

Abstract

This paper is concerned with the modelling of gear rattle in Roots blower vacuum pumps. Analysis of experimental data reveals that the source of the noise and vibration problem is the backlash nonlinearity due to gear teeth losing and re-establishing contact. We derive simple non-smooth models for the lightly damped, lightly loaded dynamics of the pump. The models include a time-dependent forcing term which arises from the eccentric mounting of the gears acting at the gross rotation rate. We use a combination of explicit construction, asymptotic methods and numerical techniques to classify complicated dynamic behaviour in realistic parametric regimes. We first present a linear analysis of permanent-contact motions, and derive upper bounds on eccentricity for silent operation. We then develop a nonlinear analysis of 'backlash oscillations', where the gears lose and re-establish contact, corresponding to noisy pump operation. We show that noisy solutions can coexist with silent ones, explaining why geared systems can rattle intermittently. Finally, we consider possible design solutions, and show implications for pump design in terms of existence and stability of solutions.

1. Introduction

Recent increases in the sizes and operating speeds of Roots blower vacuum pumps have led to intermittent noise and vibration problems in their gearing mechanism. A small amount of play between gears is essential to ensure that they will not jam. This means that there is always a gap between the trailing face of one tooth and the leading face of the next tooth, which is known as the backlash width. Because the gear wheels can consequently lose contact, there is a range of relative rotational displacements for which there is no restoring torque between the gears; this effect is known as freeplay (full details are given in Ref. [1]).

In gear systems where the load and the damping are both light, only a small amount of forcing is needed to cause rattle. Forcing due to stiffness varying at the tooth meshing frequency is well-studied, and many different models including Refs. [2,3] have been proposed to investigate this effect. These studies include multimodal analysis [4] and experimental verification of models [5].

*Corresponding author. Tel.: +44 117 331 7368; fax: +44 117 925 1154.
E-mail address: joanna.mason@bristol.ac.uk (J. Mason).

0022-460X/$ - see front matter © 2007 Elsevier Ltd. All rights reserved.
doi:10.1016/j.jsv.2007.03.071

However, motivated by experimental observation our aim is to investigate gear rattle which is caused by forcing at the rotation frequency. When compared with rattle at the tooth meshing frequency, this produces noise and vibrations with a larger amplitude at a much lower frequency; typically, at small-integer multiples of the rate of rotation. Consequently, we neglect the rapidly varying stiffness coefficient found in tooth meshing frequency models.

The main theoretical advance presented is the extension of the second-order model in Refs. [6,7], to a third-order model where the moments of inertia of the two shafts are not necessarily equal. We investigate the effect that breaking the symmetry has on the analytical bounds for the existence of various types of solution, and hence the critical eccentricity, and conclusions are drawn for machine design.

1.1. Model formulation

A typical Roots blower vacuum pump [8–11] consists of two involute steel rotors which are rigidly attached to counter-rotating parallel shafts. The X-shaft is driven by an electric motor, while the Y-shaft is driven by means of a 1:1 gearing mechanism. In quiet ('normal') operation, the gears remain in permanent linear contact (PLC), as shown in Fig. 1(a). However in noisy operation, the gears lose contact, with an audible impact when the gears re-establish contact. This is known as a backlash oscillation. There are in fact two broad types of backlash oscillations. Starting from state (a) in Fig. 1, the system can pass through state (b) (freeplay) to state (c) (torque reversal) and back again. Alternatively, the system can simply oscillate between states (a) and (b). We consider a model of two meshing spur gears and the external forces acting on the two shafts, as shown schematically in Fig. 2. The X-shaft is driven by a motor torque $T(t)$. The first harmonic of the sound generated by a noisy pump is at the same frequency as the gross rotation rate of the machine. This motivates us to seek forcing mechanisms which operate at integer multiples of the gross rotation rate. There may be

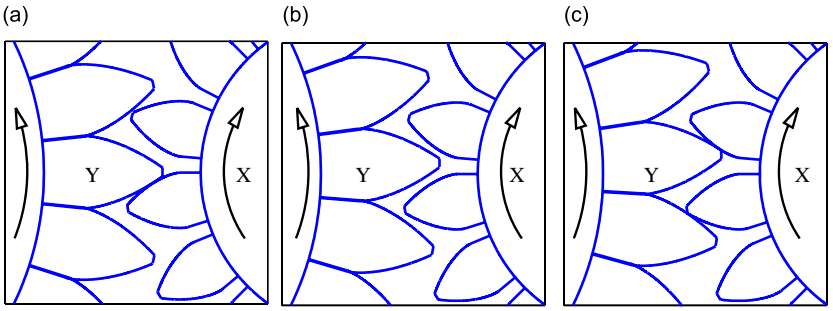

Fig. 1. The three modes of gear meshing. From left to right: (a) X drives Y, (b) freeplay, (c) Y drives X (torque reversal).

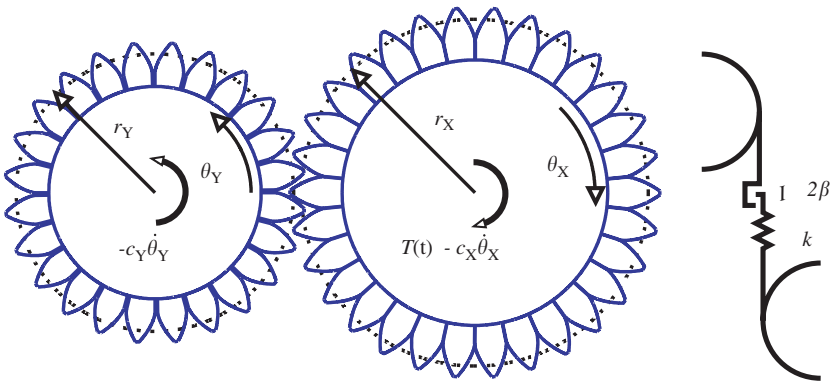

Fig. 2. The external torques acting on the shafts of meshing gears. The right-hand side drawing illustrates the interaction force between the gears.

several such mechanisms but this paper examines only two: eccentric mounting of the gears and torque ripple. Eccentricity arises when the axis of rotation is not exactly in the centre of the gear. We will show that even very small eccentricities can generate a sufficiently large forcing to drive noisy operation.

The moments of inertia of the fully assembled shafts are denoted by $I_{X,Y}$, and $r_{X,Y}$ denote the radii of the pitch circle at which contact occurs between the X and Y gears; we assume $r_X = r_Y$. The angular displacements $\theta_{X,Y}$ have directions chosen so that both coordinates increase in time. Both the X and Y-shafts suffer resistive torques against the direction of motion, given by $c_{X,Y}\dot{\theta}_{X,Y}$, where $c_{X,Y}$ are linear damping coefficients. The relative rotational displacement is defined generally by $r_X\theta_X - r_Y\theta_Y$. We also include a geometric oscillatory correction term, $e(t) = \varepsilon\cos 2\pi t$, that models the eccentric mounting of the gears. Here we focus on the special case $r_X = r_Y$, for which we work with the non-dimensional relative rotational displacement $\Theta := \theta_X - \theta_Y + e(t)$. The stiffness coefficient k is a measure of the lumped torsional rigidity of the shaft assemblies. Each gear experiences a reaction force kB, which for simplicity we assume acts normal to the shafts, and which is dependent on the relative position of the gear teeth. When the gear teeth are in contact, we use a lumped approach and suppose that each assembly deforms according to Hooke's Law. Here B is a nonlinear backlash function that consists of three linear components:

$$B(\Theta) = \begin{cases} \Theta - \beta, & \Theta > \beta \quad \text{(X drives Y)}, \\ 0, & |\Theta| < \beta \quad \text{(freeplay)}, \\ \Theta + \beta, & \Theta < -\beta \quad \text{(Y drives X)}. \end{cases} \tag{1}$$

This backlash function could be adjusted to incorporate other nonlinear effects, for example lubrication and friction, here however we leave these refinements for future work.

1.2. Equations of motion

We apply Newton's second law of motion in angular coordinates to derive equations of motion for the two shaft assemblies. For the X and Y-shaft assemblies, respectively, we have

$$I_X\ddot{\theta}_X + c_X\dot{\theta}_X + r_X kB(\theta_X - \theta_Y + e(t)) = T(t), \tag{2}$$

$$I_Y\ddot{\theta}_Y + c_Y\dot{\theta}_Y - r_Y kB(\theta_X - \theta_Y + e(t)) = 0, \tag{3}$$

where dots denote differentiation with respect to time. We model the total motor torque T by $T(t) = \overline{T} + \gamma\cos(2\pi n\tau + \xi)$, where $\overline{T}$ is the mean motor torque and γ is the amplitude of a ripple component, due to the imperfect symmetry of the armature. The mean torque $\overline{T}$ balances with the drag terms when the machine is running steadily, and so it need not be given as a separate parameter. Providing that $c_x/I_x = c_y/I_y$ we can reduce Eqs. (2) and (3) to a single non-autonomous second-order differential equation for the relative rotational displacement measured at the pitch circle $\Phi = \theta_X - \theta_Y + e(t)$. By non-dimensionalising with the rotation period, we find that

$$\Phi'' + \delta\Phi' + 2\kappa B(\Phi) = 4\pi\delta - 4\pi^2\varepsilon\cos(2\pi\tau) - 2\pi\delta\varepsilon\sin(2\pi\tau) + \gamma\cos(2\pi n\tau + \xi), \tag{4}$$

where $'$ denotes differentiation with respect to non-dimensional time τ. We note that the rescaled damping δ, half-backlash width β and eccentricity parameter ε are good candidates for use as small parameters in perturbation analysis and that $\delta \sim \beta \sim \varepsilon$. In comparison, the rescaled stiffness parameter κ is large.

The ripple component γ is very small compared to the mean motor torque $4\pi\delta$, therefore, for the remainder of our work we neglect torque ripple and concentrate on the effect of eccentricity only.

1.3. Two degree of freedom dimensionless model

The single degree of freedom (dof), second-order, model requires that the ratio of the moments of inertia and damping coefficients of the X and Y-shafts are equal. We now extend the scope of our model by allowing the quantities to differ; in this case, θ_X and θ_Y are independent coordinates. For algebraic convenience we

choose a non-dimensional parameter $\eta \in (-1, 1)$, to measure the broken symmetry, so that

$$\frac{I_X}{\overline{I}} = 1 + \eta, \quad \text{and} \quad \frac{I_Y}{\overline{I}} = 1 - \eta, \quad \text{where } \overline{I} = \frac{I_X + I_Y}{2}. \tag{5}$$

After non-dimensionalisation, it is possible to re-write the pair of coupled second-order ODEs as a system of three first-order equations by introducing new coordinates, (Φ, Ψ, Z), where $\Phi = \theta_x - \theta_y + e(t)$ as before, $\Psi = \Phi'$ and $Z = \theta'_X + \theta'_Y$. We now have

$$\begin{pmatrix} 1 & 0 & 0 \\ 0 & 1 & \eta \\ 0 & \eta & 1 \end{pmatrix} \begin{pmatrix} \Phi' \\ \Psi' \\ Z' \end{pmatrix} = \begin{pmatrix} 0 & 1 & 0 \\ 0 & -\delta & 0 \\ 0 & 0 & -\delta \end{pmatrix} \begin{pmatrix} \Phi \\ \Psi \\ Z \end{pmatrix} + \begin{pmatrix} 0 \\ 4\pi\delta + e'' + \delta e' - 2\kappa B(\Phi) \\ 4\pi\delta + \eta e'' \end{pmatrix}. \tag{6}$$

The scaling is such that δ, ε and κ take the same values as for the one dof model.

2. Permanent linear contact solutions

Solutions where the gears remain permanently in contact are highly desirable; we wish to find bounds on parameters for their existence. Eq. (4) for Φ in the PLC region is linear and can be solved exactly. We must then apply an *a posteriori* check for the validity of solutions, namely that $\Phi(\tau) > \beta$ for all τ. This provides us with a bound for eccentricity:

$$\varepsilon < \varepsilon_{\text{crit}}^{\text{1dof}} := \frac{2\delta}{\kappa} \sqrt{\frac{(\kappa - 2\pi^2)^2 + \pi^2\delta^2}{4\pi^2 + \delta^2}}, \tag{7}$$

above which silent solutions are destroyed. As $\kappa \to \infty$ (motivated by physical parameters of real machines) we have

$$\varepsilon_{\text{crit}} \sim \frac{\delta}{\pi} + O(\delta^3). \tag{8}$$

Typical measured eccentricities are of the same order of magnitude as the calculated critical eccentricity. This could explain the experimental observations that the same machine can behave inconsistently and 'identical' machines behave differently since the PLC solution can be eliminated with a small change in the machine parameters. Increasing inertia, however, decreases δ and will make rattle more likely; we therefore wish to find design solutions to increase $\varepsilon_{\text{crit}}$. It has been suggested [12] that breaking the symmetry of the system by removing mass may be used to increase $\varepsilon_{\text{crit}}$. We now proceed to examine this idea.

We write Eq. (6) in the form:

$$\mathbf{M}\mathbf{u}' = \mathbf{A}\mathbf{u} + \mathbf{b}_1 - \text{Re}\{\mathbf{b}_2 \exp 2\pi\tau \text{i}\}, \tag{9}$$

where Re denotes the real part, i the square root of -1 and $e(\tau) = \text{Re}\{\varepsilon \exp 2\pi\tau\text{i}\}$ is the eccentricity term. We solve Eq. (9), and apply the *a posteriori* check to find the bound

$$\varepsilon < \varepsilon_{\text{crit}}^{\text{2dof}} = \frac{2\delta}{\kappa} \sqrt{\frac{((\kappa - 2\pi^2)^2 + \pi^2\delta^2) + \dfrac{8\pi^4\eta^2}{4\pi^2 + \delta^2}\,(2(\kappa - 2\pi^2) + \delta^2 + 2\pi\eta^2)}{(4\pi^2 + \delta^2) + \dfrac{8\pi^2\eta^2}{4\pi^2 + \delta^2}\,((4\pi^2 - \delta^2) - 2\pi^2\eta^2)}} \tag{10}$$

for the existence of PLC solutions. Note that for $\eta = 0$, $\varepsilon_{\text{crit}}^{\text{2dof}} = \varepsilon_{\text{crit}}^{\text{1dof}}$ as required. Expanding Eq. (10) as a binomial series in small η, for fixed δ and κ, gives

$$\varepsilon_{\text{crit}} = \varepsilon_{\text{crit}}^{\text{1dof}}(1 + \eta^2 + O(\eta^4)). \tag{11}$$

Hence for small η, breaking the symmetry by removing mass from one shaft and adding it to the other increases $\varepsilon_{\text{crit}}$ (a desirable effect). The advantage of the η parameter is that it allows easy manipulation of the equations of motion and does not change the values of the other non-dimensional parameters. However it is more physically interesting to investigate the effect of adding/removing mass to just one shaft, or equally to

both shafts. We thus introduce two new non-dimensional variables μ and v: μ measures half the ratio of mass added/removed to *either one of* the X or Y-shafts, while v measures half the ratio of mass added/removed to *each* shaft. Note that the parameters v and μ result in the same total change in mass.

We substitute expressions for μ and v into Eq. (10) (with suitably modified damping and stiffness parameters due to the change in total mass) and then expand as a binomial series in small μ, v, respectively, for fixed δ and κ as above, to give

$$\varepsilon_{\text{crit}} = \varepsilon_{\text{crit}}^{1\text{dof}}(1 - \mu + 2\mu^2 + O(\mu^3)), \tag{12}$$

and

$$\varepsilon_{\text{crit}} = \varepsilon_{\text{crit}}^{1\text{dof}}(1 - v + v^2 + O(v^3)). \tag{13}$$

Thus (for small μ and v) it is better to remove mass from one shaft rather than half the amount of mass from both the X and Y-shafts, but the improvement is a second-order effect.

3. Conditions for noisy operation

Numerical simulations of the initial value problems Eqs. (4) and (6) reveal a very rich structure of coexisting stable solutions. Analysis for the one dof model shows that there are many stable rattling periodic orbits that can coexist with quiet operation. Simulations suggest that this is also true in the two dof model; some outputs are shown in Fig. 3 for realistic machine parameters where a variety of different initial data have been chosen. For some parameter values it seems that noisy solutions predominate. For certain choices of machine parameters we would like to understand whether it is possible to destroy the noisy solutions. In these solutions, the majority of time is spent in freeplay. The large stiffness value κ results in impact-like events of short duration, where the gears make contact. We approximate the contact as a pure impact [13] through a classical coefficient of restitution law (with coefficient of restitution = 1). It was shown in Refs. [6,7] that, to leading order, existence and stability criteria are identical for the finite and infinite stiffness models in the limit $\kappa \to \infty$, thus for convenience we consider only the impacting model of backlash here. Thus the only differential equation we need solve is Eq. (6) in the freeplay region, where $B(\Phi) = 0$, though the problem is still harshly nonlinear due to impacts.

We use the notation introduced in Refs. [6,7] to identify different types of periodic solution. We let $P(m, n^+, n^-)$ denote a periodic solution, of period $m \in \mathbb{Z}$, where $n^{\pm}$ denote the number of times per period that the orbit contacts the $\Phi = \pm\beta$ boundaries, respectively.

3.1. $P(m, 1, 0)$ solutions

We begin by considering solutions of type $P(m, 1, 0)$, which repeat once every m periods of the forcing, hit the $\Phi = +\beta$ boundary once per period and never contact the $\Phi = -\beta$ boundary (see Fig. 4). Our general method for solution construction is as follows. We solve the differential equation (6) in the freeplay region and find explicit expressions for Φ, Ψ and Z (with three constants of integration which we label c_1, c_2 and c_3; see Ref. [14]). We then patch solution segments together with the impact and periodicity conditions. With reference to Fig. 4 our solution loses contact with the $+\beta$ boundary at some initial unknown time σ, with velocity $-v$; the periodicity condition then implies that our solution impacts the $+\beta$ boundary again at some time $\sigma + m$ with velocity v. Hence:

$$\Phi(\sigma) = \beta, \quad \Psi(\sigma) = -v, \tag{14}$$

$$\Phi(\sigma + m) = \beta, \quad \Psi(\sigma + m) = v. \tag{15}$$

Conservation of angular momentum also implies that

$$Z(\sigma) = Z(\sigma + m) + 2\eta v. \tag{16}$$

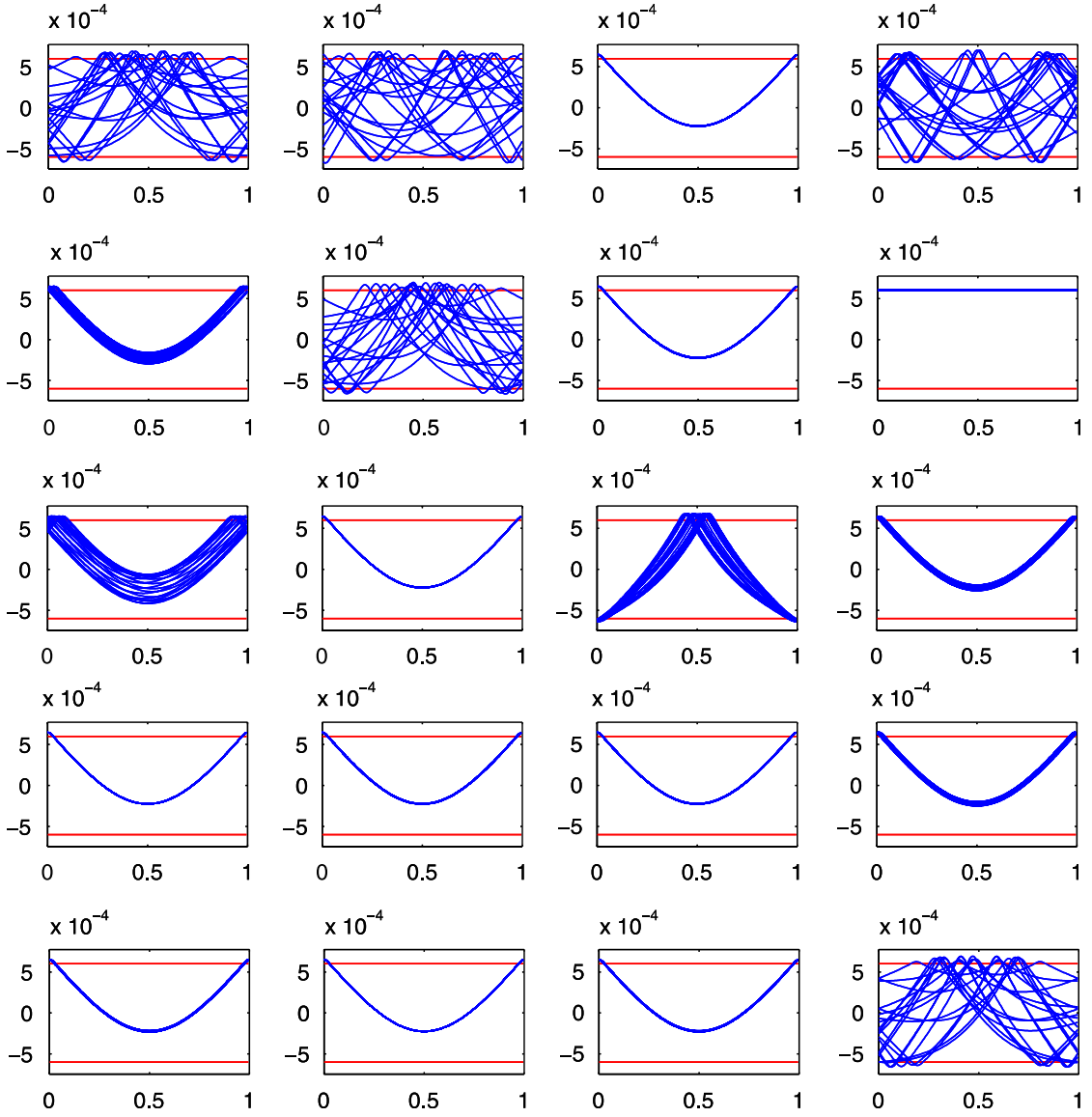

Fig. 3. Numerical simulations of the initial value problem for the two degree of freedom model for identical machine parameters (for which silent PLC solutions exist), and an ensemble of initial conditions. Each graph is a plot of relative rotational displacement $\Phi(\tau)$ against τ, plotted over the last 20 periods of forcing, with $\Phi = \pm\beta$ shown as horizontal lines. These show a mixture of noisy solutions and 'less noisy' single contact solutions. Note that there is only one permanent linear contact solution shown in column 4, row 2 (the solution curve is indistinguishable from $\Phi = \pm\beta$ because of the vertical scale).

By applying conditions Eqs. (14)–(16) we obtain a system in the form, $\mathbf{Ac} = \mathbf{b}$ to solve for the five unknowns c_1, c_2, c_3, v and σ,

$$\begin{pmatrix} 1 & e_\sigma^- & e_\sigma^+ & 0 \\ 1 & e_m^- & e_m^+ & 0 \\ 0 & \lambda_- e_\sigma^- & \lambda_+ e_\sigma^+ & 1 \\ 0 & \lambda_- e_m^- & \lambda_+ e_m^+ & -1 \\ 0 & \lambda_-(e_m^- - e_\sigma^-) & \lambda_+(e_\sigma^+ - e_m^+) & -2\eta \end{pmatrix} \begin{pmatrix} c_1 \\ c_2 \\ c_3 \\ v \end{pmatrix} = \begin{pmatrix} \beta - 4\pi\sigma - \varepsilon\cos 2\pi\sigma \\ \beta - 4\pi(\sigma + m) - \varepsilon\cos 2\pi\sigma \\ -4\pi + 2\pi\varepsilon\sin 2\pi\sigma \\ -4\pi + 2\pi\varepsilon\sin 2\pi\sigma \\ 0 \end{pmatrix}, \tag{17}$$

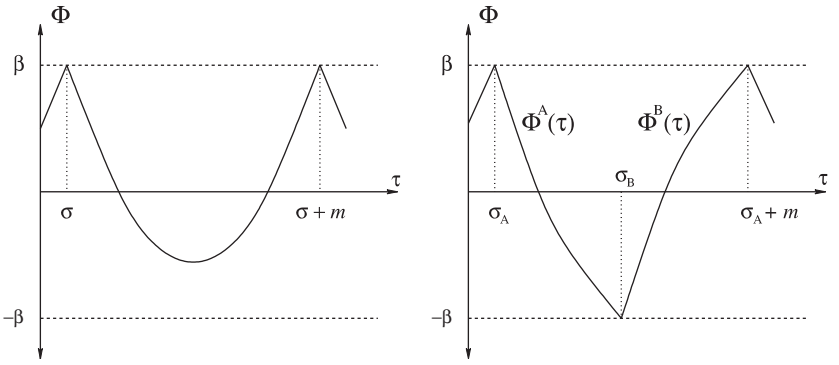

Fig. 4. Sketches of $P(m,1,0)$ and $P(m,1,1)$ orbits, respectively. The LHS picture illustrates the impacts at the $+\beta$ boundary, at unknown times σ and $\sigma+m$. The RHS picture illustrates the $\pm\beta$ impacts at σ_A and σ_B, respectively.

where $\mathbf{c}=[c_1\,c_2\,c_3]^{\mathrm{T}}$, $\lambda_\pm=-\delta/(1\pm\eta)$, $e_\sigma^\pm=e^{-\lambda_\pm\sigma}$ and $e_m^\pm=e^{-\lambda_\pm(\sigma+m)}$. We then find a matrix $\mathbf{P}$ such that $\mathbf{PA}$ is in echelon form, which gives us expressions for c_1, c_2, c_3 and v, and generates an algebraic constraint on the impact time σ.

3.2. Existence and stability of solutions

Following the above procedure, we find that the impact time σ takes the form

$$\sigma=\frac{1}{2\pi}\sin^{-1}\left[\frac{1}{\varepsilon}\left(2-\frac{\lambda_- m}{2}\coth\left(\frac{\lambda_- m}{2}\right)-\frac{\lambda_+ m}{2}\coth\left(\frac{\lambda_+ m}{2}\right)\right)\right]. \tag{18}$$

There are two admissible solutions to Eq. (18); we expand them in terms of the small parameter δ to give:

$$\sigma=\begin{cases}\dfrac{-\delta^2m^2(1+\eta^2)}{12\pi\varepsilon(1-\eta^2)^2}+O(\delta^4): & \text{in phase solution,}\\[2ex] \dfrac{1}{2}+\dfrac{\delta^2m^2(1+\eta^2)}{12\pi\varepsilon(1-\eta^2)^2}+O(\delta^4): & \text{out of phase solution.}\end{cases} \tag{19}$$

Numerical evidence indicates that the in phase solution is stable, and the out of phase solution is unstable. The $P(m,1,0)$ solutions do not exist if the argument of the arcsin function in Eq. (18) exceeds one in modulus.

This gives us a condition on eccentricity:

$$\varepsilon>\varepsilon_{\mathrm{crit}}:=\frac{\delta^2m^2(1+\eta^2)}{6(1-\eta^2)}+O(\delta^4), \tag{20}$$

for the existence of simple $P(m,1,0)$ solutions. Since in practice ε and δ are of similar magnitude, this bound will always be satisfied for realistic parameters and hence it is very difficult to eliminate rattling solutions by reducing eccentricity, and moreover, the $\varepsilon\sim\mathcal{O}(\delta^2)$ scaling is independent of the symmetry breaking parameter η.

We must also check that the solution trajectory does not hit the boundary $\Phi=-\beta$. To determine this we must find the minimum displacement; we thus require $\hat\tau$ such that $\Phi'(\hat\tau)=\Psi(\hat\tau)=0$; we try a power series solution in the form

$$\hat\tau=\sigma+\frac{m}{2}+\hat\tau_0+\hat\tau_1\delta+O(\delta^2). \tag{21}$$

We have four cases corresponding to in phase/out of phase solution and m odd/even. In each case we solve for the coefficients $\hat\tau_i$, substitute these expressions for $\hat\tau$ into the condition $\Phi(\hat\tau)>-\beta$ and expand this as a series as

well. For the in phase solution ($\sigma \approx 0$) not to contact the lower boundary we require

$$\beta > \begin{cases} \varepsilon + \dfrac{\pi m^2 \delta}{4(1-\eta^2)} + O(\delta^2): & m \text{ odd}, \\ \dfrac{\pi m^2 \delta}{4(1-\eta^2)} + O(\delta^2): & m \text{ even}, \end{cases} \tag{22}$$

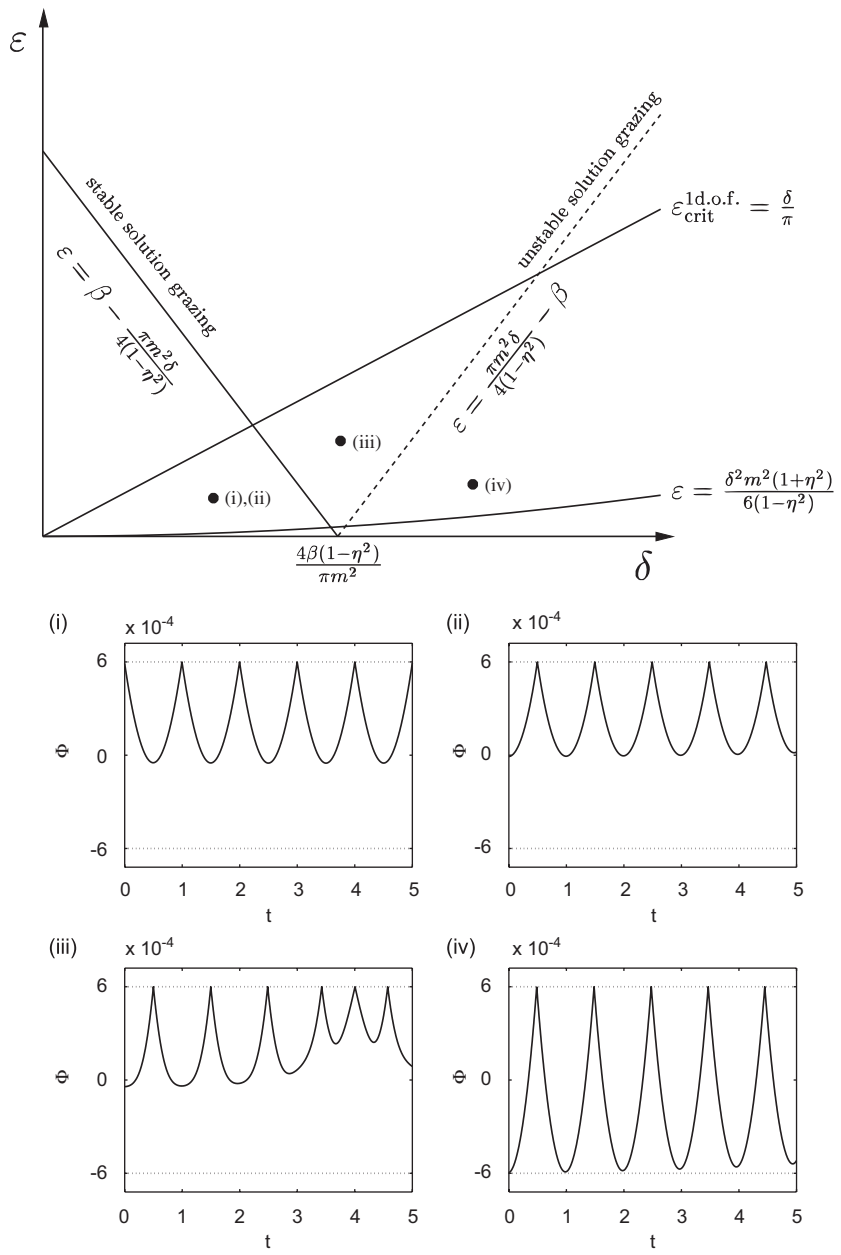

Fig. 5. Sketch of the existence bounds for the $P(m,1,0)$ solutions (in the case $m=1$ and $\eta=0$). The bounds (22) and (23) describe the stable and unstable solution grazings with $\Phi = -\beta$, respectively. The critical eccentricity bound is also shown. (i)–(iv) are numerical integrations of Eq. (4) in the freeplay region. The parameter values chosen are shown schematically on the bifurcation diagram. (i) and (ii) illustrate coexisting in phase and out of phase $P(m,1,0)$ solutions, respectively. (iii) illustrates an unstable out of phase $P(m,1,0)$ solution and (iv) illustrates an unstable out of phase $P(m,1,1)$ solution.

and for the out of phase solution ($\sigma \approx \frac{1}{2}$) not to contact the lower boundary we require

$$\beta > \begin{cases} \dfrac{\pi m^2 \delta}{4(1-\eta^2)} - \varepsilon + O(\delta^2): & m \text{ odd}, \\ \dfrac{\pi m^2 \delta}{4(1-\eta^2)} + O(\delta^2): & m \text{ even}. \end{cases} \tag{23}$$

Note that when the symmetry breaking parameter $\eta = 0$ we recover the bounds for the one dof model. In Fig. 5 we have plotted the existence bounds found in Eqs. (20), (22) and (23) in the eccentricity damping plane. From this we conclude that increasing η increases the bounds on ε though this is only a higher order effect.

3.3. $P(m, 1, 1)$ *solutions*

We now proceed to show how one might examine noisier, less desirable solutions of type $P(m, 1, 1)$ that visit all three regimes, thus impacting both $\pm\beta$ boundaries. The overall aim is to find existence bounds for these noisy solutions, and therefore determine how they can be eliminated. We write the solution Φ as the combination of two parts so that

$$\Phi(\tau) = \begin{cases} \Phi^A(\tau), & \sigma_A < \tau < \sigma_B, \\ \Phi^B(\tau), & \sigma_B < \tau < \sigma_A + m \end{cases} \tag{24}$$

(and similarly for Ψ and Z); see Fig. 4. σ_A and σ_B denote the impact times with the $\pm\beta$ boundaries, respectively. Similarly to before, we can patch our solution segments together with the impact and periodicity conditions.

We find that the expressions for $\sigma_{A,B}$ are not solvable in closed form, it is necessary to resort to a numerical root finding procedure to find the impact times. Once the solutions have been found, as for the $P(m, 1, 0)$ case, a retrospective check has to be made to ensure that the constructed solution is always in the correct regime. The aim would then be to find conditions on the symmetry-breaking parameters, to determine how this noisy type of solution can be destroyed and replaced by quieter single-contact solutions. This analysis remains for future work. We can, however, determine stability numerically using an initial value solver written in MATLAB. Some outputs are shown in Fig. 5.

4. Conclusions

In this paper we have considered a mathematical model of noise and vibration in lightly damped lightly loaded Roots blower vacuum pumps. We have extended the work carried out by Halse et al. [6,7], by constructing a full two dof model, and investigated the effects of breaking the symmetry between the two shafts. In particular, we derived analytical bounds for the existence of various classes of periodic solution as a function of parameters. We discovered that removing mass from the system increases the critical value of eccentricity (below which silent solutions exist), whilst adding mass reduces this existence bound. Unfortunately, one is very limited in how much mass one can remove from such a machine, without compromising its structural integrity.

Future work should expand the work of Section 3 into a formal bifurcation analysis and compute basins of attraction, i.e. which starting configurations end up at which (stable) periodic solutions. Much work also remains to be done in experimental validation and investigation of other design solutions. Mathematical models of these new types of system will involve more degrees of freedom and will be more complicated than any existing mathematical treatment of backlash systems.

Acknowledgements

The authors gratefully acknowledge the support of a CASE award from BOC Edwards Ltd. and the Engineering and Physical Sciences Research Council.

References

[1] H.E. Merritt, *Gear Engineering*, Pitman Publishing, 1971.
[2] S. Theodossiades, S. Natsiavas, Non-linear Dynamics of gear-pair systems with periodic stiffness and backlash, *Journal of Sound and Vibration* 229 (2000) 287–310.
[3] G. Blankenship, A. Kahraman, Steady state forced response of a mechanical oscillator with combined parameter excitation and clearance nonlinearity, *Journal of Sound and Vibration* 185 (1995) 743–765.
[4] H. Vinayak, R. Singh, Multi-body dynamics and modal analysis of compliant gear bodies, *Journal of Sound and Vibration* 210 (1998) 171–214.
[5] A. Kahraman, G. Blankenship, Effect of involute contact ratio on spur gear dynamics, *Journal of Mechanical Design* 121 (1999) 112–118.
[6] C.K. Halse, Nonlinear Dynamics of the Automotive Driveline, PhD Thesis, University of Bristol, 2004.
[7] C.K. Halse, R.E. Wilson, M.E. Homer, M. di Bernardo, Coexisting solutions and bifurcations in mechanical oscillators with backlash. *Journal of Sound and Vibration*, 2007, in press, doi:10.1016/j.jsv.2007.05.010.
[8] M.H. Hablanian, Design and performance of oil-free pumps, *Vacuum* 41 (1990) 1814–1818.
[9] W.T. Holmes, *Plane Geometry of Rotors in Pumps and Gears*, The Scientific Publishing Company, 1978.
[10] A.P. Troup, N.T.M. Dennis, Six years of "dry pumping": a review of experiences and issues, *Journal of Vacuum Science and Technology* A 9 (1990) 2048–2052.
[11] H. Wycliffe, Mechanical high-vacuum pumps with oil-free swept volume, *Journal of Vacuum Science and Technology* A 5 (1987) 2608–2611.
[12] T. Davenne, BOC Edwards Ltd, Personal communications.
[13] K. Karagiannis, F. Pfeiffer, Theoretical and experimental investigations of gear-rattling, *Nonlinear Dynamics* 2 (1991) 367–387.
[14] J.F. Mason, Mathematical Modelling of Gear Rattle in Dual-shaft Vacuum Pumps, Master's Thesis, University of Bristol, 2004.